Proceedings of the Institute of Acoustics

# AUTOMATIC CONTROL OF BOUNDARY LAYER TRANSITION USING A DOUBLE SUCTION PANEL

J -L RIOUAL, P A NELSON, M J FISHER

Institute of Sound and Vibration Research, Southampton University, Southampton SO9 5NH, ENGLAND.

## 1. INTRODUCTION

Reducing the skin friction drag of transonic commercial aircraft has always stimulated research in aerodynamics. The basic principal in boundary layer drag reduction is to delay the transition region where the boundary layer undergoes a change from laminar state to turbulent state. As reported by Gad-el-Hak [1] several methods to delay transition have been tested in the past, among which are the use of flexible coating, suction, shaping and wall-cooling. Among these methods, suction has established its practicality for aircraft application thanks to real flight tests [2]. The manufacture of laser drilled titanium sheets makes the installation of suction panels easier with minimum roughness induced instabilities. Two major problems that remain to be solved in the use of boundary layer suction, are the distribution and optimisation of suction [1]. The use of automatic adaptive control of suction seems to offer a practical solution to such problems. The continuous monitoring of the boundary layer by adjusting individual suction rates to keep the flow laminar at minimum power penalty will allow to reduce the total power involved in the propulsion of aircraft, and will make tests in expensive high speed wind tunnels shorter and more economic by reducing significantly the time and the uncertainty of the manual adjustment of individual suction rates. The work presented in this paper is the continuation of the experimental investigations reported in [3] where it was shown that a feedback control loop could be used to maintain transition of a flat plate boundary layer at a desired location downstream of a suction panel, using surface pressure fluctuation measurements as indicators of the transition region. The experimental results described here show that an optimal feedback control loop can be used to fix transition at a desired location with minimum power penalty by permanently adjusting the suction rates of two individual pumps. The behaviour of the system with two suction inputs and the aim of the controller are firstly described. The approach towards the constrained optimisation problem is then presented and the controller outputs are derived. The first experimental results using the controller are then presented.

## 2. DOUBLE SUCTION INPUT AND EFFECT OF PRESSURE GRADIENT

A flat plate with a carefully machined leading edge was positioned in a wind tunnel with a 2.5 metre long 0.305 m × 0.23 m working section, allowing mean flow velocities up to 22 m $s^{-1}$ with 1% turbulence level. Two 0.124 chord × 0.178 span suction panels were mounted on the plate at positioned chosen according to hot wire anonometry measurements. Each suction panel was connected to a pump which is controlled by a PC via an inverter. The surface pressure fluctuation measurements were made downstream of the suction panels using an array of electret microphones mounted underneath a 1 mm hole, the microphone signals were acquired by a PC via an A/D interface board. In order to remove the effect of the fan noise on the

pressure measurements, the microphone signals were high pass filtered at 800 Hz. Figure 1 shows a sketch of the equipment used.

The signals were acquired for 0.1 s at a sampling rate of 4 kHz after which the rms values of the signals were calculated. These values were then normalised by the rms pressure measured for a fully turbulent boundary layer, hence yielding a value close to zero in the laminar region and a value close to one in the turbulent region. In order to monitor the location of transition, four normalised rms pressures were used to create an error signal given by

$$e(k) = \sum_{m=1}^{4} [p_r(x_m) - p(x_m, k)] \qquad (1)$$

where $p(x_m, k)$ is the normalised rms pressure at position $x_m$ on the plate at the k'th control cycle, and $p_r(x_m)$ is the desired rms pressure at position $x_m$.

With the desired pressures chosen to be $p_r(x_1) = 0.2$, $p_r(x_2) = 0.33$, $p_r(x_3) = 0.66$ and $p_r(x_4) = 0.8$, the error signal $e(k)$ gives a value close to $-2$ when the boundary layer is already turbulent at $x_1$, a value close to 2 when the boundary layer is still laminar at $x_4$, and a value close to 0 when transition occurs between $x_1$ and $x_4$. Varying the suction rates on both panels from minimum to maximum and measuring the ensemble averaged relationship between the steady state error signal $e(k)$ and the values of the voltages output to the suction pump controllers gives a good idea of the effect of suction on the error. Figure 2 shows for a given mean flow speed, $U_o = 17.5$ m s$^{-1}$, the contour plot of the steady state error $e(k)$ as a function of the steady state values of the inputs $u_1(k)$ and $u_2(k)$, voltages to the suction pump speed controllers corresponding to the suction panel 1 (upstream) and the suction panel 2 (downstream) respectively. As shown by figure 2, there is an infinite distribution of suction that will give zero error, $e(k) = 0$. The suction distribution giving zero error for the minimum power penalty is however unique, and this is the target point of the controller as shown by the shaded circle in figure 2. The contour plot described here was measured in the case of the flat plate without pressure gradient, and this explains why the zero error point with minimum power penalty corresponds to equal suction on both suction panels. The effect of a pressure gradient on the plate can be seen in figure 3 which shows the same experiments as in figure 2 but this time an additional plate was used in the wind tunnel to induce a favourable pressure gradient on the first suction panel and an adverse pressure gradient on the second suction panel. This case represents in a simple manner the type of pressure distribution that would exist near the leading edge of an aerofoil. As shown in figure 3, the error contour is now different and it leads to a different target point of zero error with minimum power penalty. The target now corresponds to an increased suction rate for the second panel and a decreased suction rate for the first panel. As it will be shown in section 4, the two different configurations of figures 2 and 3 will lead to a different adjustment of the controller outputs.

## 3. A SELF-TUNING CONTROLLER FOR SUCTION RATE OPTIMISATION

As explained in the previous section, in order to achieve the target points of zero error and minimum power input to the pumps, the controller will need to update the pump control voltages $u_1(k)$ and $u_2(k)$ in order to fulfil the conditions

$$e(k+1) = 0 \tag{2}$$

$$min(u_1(k)^2 + u_2(k)^2) \tag{3}$$

As explained in reference 4 such a constrained problem can be converted into an unconstrained problem of the form

$$J(k) = u_1(k)^2 + u_2(k)^2 + \lambda(k+1)\, e(k+1) \tag{4}$$

where $\lambda(k+1)$ is the Lagrange multiplier [4].

The method used here to minimise the cost function $J(k)$ is to update the control voltages $u_1(k)$ and $u_2(k)$ according to the steepest descent algorithm defined by

$$\begin{pmatrix} u_1(k+1) \\ u_2(k+1) \end{pmatrix} = \begin{pmatrix} u_1(k) \\ u_2(k) \end{pmatrix} - \mu\, grad(J(k))_{(u_1(k),\, u_2(k))} \tag{5}$$

and the Lagrange multiplier $\lambda(k+1)$ is updated as a predictor of the error function driven to zero at the next iteration, i.e.

$$e(k+2) = 0 \tag{6}$$

Details of the derivation of the algorithm are given in reference 5. In order to derive the exact expression of the gradient of the cost function and the analytical expression of the controller update a valid model of the system giving the error as a function of the two control voltages is needed. The response of the error $e(k)$ to step inputs has shown that the dynamics of the plant can be modelled by a two input/single output system governed by the difference equation

$$e(k+1) = a_1(k)\, u_1(k) + a_2(k)\, u_2(k) + b(k) + w(k+1) \tag{7}$$

where $a_1(k)$, $a_2(k)$ and $b(k)$ are the parameters of the model and $w(k+1)$ is an additional disturbance representing the noise of the error signal.

Replacing the above expression for $e(k+1)$ into equation 4 allows the gradient of $J(k)$ with respect to $u_1(k)$ and $u_2(k)$ to be calculated and equation 5 can finally be rewritten as

$$\begin{pmatrix} u_1(k+1) \\ u_2(k+1) \end{pmatrix} = \begin{pmatrix} u_1(k) \\ u_2(k) \end{pmatrix} - \mu \begin{pmatrix} 2\, u_1(k) + a_1(k)\, \lambda(k+1) \\ 2\, u_2(k) + a_2(k)\, \lambda(k+1) \end{pmatrix} \tag{8}$$

Assuming that the parameters of equation 7 can be used in a predictor for the next iteration, the noise free expression of equation 6 can be written

$$e(k+2) = a_1(k)\, u_1(k+1) + a_2(k)\, u_2(k+1) + b(k) = 0 \tag{9}$$

Substituting $u_1(k+1)$ and $u_2(k+1)$ given by equation (8) leads to the analytical expression of $\lambda(k+1)$ given by

$$\lambda(k+1) = \frac{(1-2\mu)\,(a_1(k)\,u_1(k) + a_2(k)\,u_2(k)) + b(k)}{\mu(a_1(k)^2 + a_2(k)^2)} \tag{10}$$

Replacing $\lambda(k+1)$ into equation 8 leads to the control update

$$\begin{pmatrix} u_1(k+1) \\ u_2(k+1) \end{pmatrix} = (1-2\mu) \begin{pmatrix} u_1(k) \\ u_2(k) \end{pmatrix} - \frac{(1-2\,\mu)\,(a_1(k)\,u_1(k) + a_2(k)\,u_2(k) + b(k))}{a_1(k)^2 + a_2(k)^2} \begin{pmatrix} a_1(k) \\ a_2(k) \end{pmatrix} \tag{11}$$

As shown in figure 2, the steady state relationship between the error signal and the two pump control voltages is dependent on the local values of the two voltages. This is also true for the dynamic model of the plant represented by equation 7. The values of $a_1(k)$, $a_2(k)$ and $b(k)$ depend on the values of $u_1(k)$ and $u_2(k)$ and whenever $u_1(k)$ and $u_2(k)$ vary, so must $a_1(k)$, $a_2(k)$ and $b(k)$. A recursive least squares (RLS) algorithm is used in the control loop to allow the model parameters to be updated at each iteration, when new data becomes available. The step of identification used here allows a valid model of the plant to be used in order to derive a reliable control update. The RLS algorithm is explained in detail in reference 6. As also supported in reference 6, the RLS algorithm has to be used with caution because of possible numerical instability of the algorithm, slow response to significant parameter changes and unidentifiability of the system. Such problems were treated using the Burman U-D factorization, a variable forgetting factor and an additional dither signal on the inputs $u_1(k)$ and $u_2(k)$. Details of these modifications are thoroughly treated by Wellstead and Zarrop [6] and Fortescue et al [7] for the use of the variable forgetting factor.

## 4. RESULTS

During the first iterations of system identification, the RLS algorithm often gives large amplitude variations of the parameters before these can converge. This initial adjustment may lead to controller instabilities when both $a_1(k)$ and $a_2(k)$ lead to a null denominator in equation 11. This problem was easily dealt with by runing the RLS identification for an initial 40 iterations during which no control action was applied. During this time, the plant was submitted to two steady voltages with additional dithers as inputs. Such large amplitude variations may also occur when the system to be identified go through non-linear variations that can not be efficiently dealt with by a linear estimation process like the RLS algorithm. In our case, sudden changes of the mean flow speed of the wind tunnel could lead to such non-linear variation of the model. In this situation the resulting large amplitude error $e(k)$ crossing a given threshold was used to switch the controller to an integral action of the form

$$\begin{pmatrix} u_1(k+1) \\ u_2(k+1) \end{pmatrix} = \begin{pmatrix} u_1(k) \\ u_2(k) \end{pmatrix} - K \begin{pmatrix} e(k+1) \\ e(k+1) \end{pmatrix} \tag{12}$$

The RLS algorithm was then reinitialised and left to converge for 40 iterations with the last integral update as input. After these 40 iterations the constrained optimisation action of equation 11 was reactivated.

The two time histories depicted in figure 4 show the behaviour of the controller in the case of the flat plate without pressure gradient. It can clearly be seen how the controller adjusts the control voltages after the initial identification iterations and how the sudden change in mean flow speed from $U_o = 14$ m s$^{-1}$ to $U_o = 17$ m s$^{-1}$ is negotiated. Plotting the data of figure 4 in the same format as in figures 2 and 3 allows one to visualise how the controller distributes the suction rates on the two panels (figure 5). Figure 6 shows in the same way as figure 5 the controller behaviour in the case of the flat plate with the additional pressure gradient. Comparing figure 5 and 6 shows the effect of the pressure gradient which generally increases the overall suction rates and distributes more suction to the second panel as could be predicted by the steady state plots of figures 2 and 3.

## 5. CONCLUSION

These first wind tunnel experiments have clearly shown how a constrained optimisation algorithm with variable Lagrange multiplier can be used in a feedback control loop to maintain transition at a desired location with minimum power penalty on the two suction pumps. The parameters of the model identified using a modified RLS algorithm could be used to create a one-step-ahead adaptive controller. The experiments have shown the fast and stable rate of convergence of the controller in the two cases, the flat plate configuration where the target was equal suction on both panels, and the pressure gradient configuration where the target was a decreased suction rate on the first panel submitted to a favourable pressure gradient and an increase suction rate on the second panel submitted to an adverse pressure gradient.

## 6. REFERENCES

[1] Gad-el-Hak M, 'Flow Control', Applied Mechanics Review, vol 42, no. 10, p.261-293 (1989).
[2] Arnal D, 'Boundary Layer Transition: Prediction, Application to Drag Reduction', AGARD Report no 786 (1992).
[3] Nelson P A, Rioual J-L and Fisher M J, 'Experiments on the Active Control of Boundary Layer Transition', Proceedings of the DGLR-AIAA Conference on Aero-Acoustics, Aachen (1992).
[4] Adby P R & Dempster M A H, Introduction to Optimization Methods, Chapman and Hall, London, p.119-126 (1974).
[5] Nelson P A, Rioual J-L and Fisher M J, 'An Algorithm for the Constrained Adaptive Control of Multiple Input - Single Output Non-Linear Systems', ISVR Technical Memorandum no 722 (1993).
[6] Wellstead P E and Zarrop M B, Self-Tuning Systems, John Wiley, Chichester (1991).
[7] Fortescue T R, Kershenbaum L S and Ydstie B E, 'Implementation of Self-tuning Regulators with Variable Forgetting Factors', Automatica, vol 17, no 6, p.831-835 (1981).

## AUTOMATIC CONTROL OF BOUNDARY LAYER TRANSITION

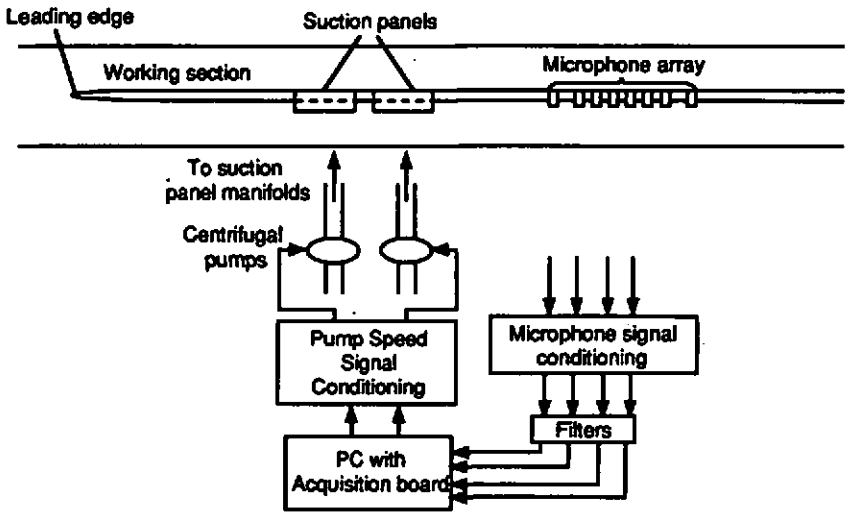


Figure 1: Schematic of test rig and double suction control equipment

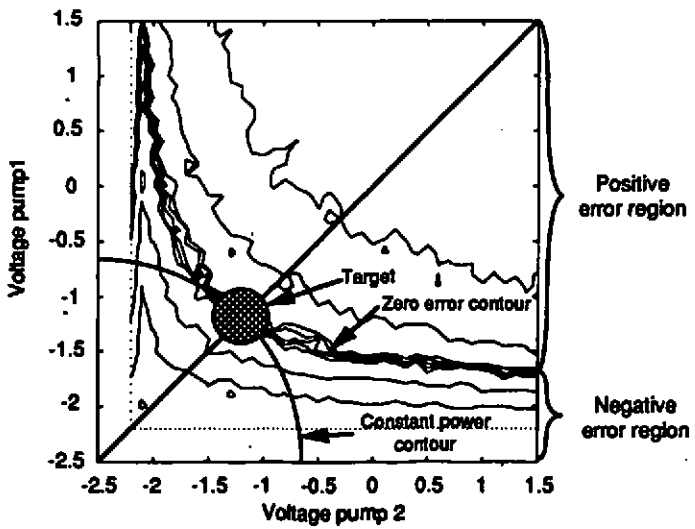


Figure 2: Contour Plot of the Error Surface in the Case of Zero Pressure Gradient

## AUTOMATIC CONTROL OF BOUNDARY LAYER TRANSITION

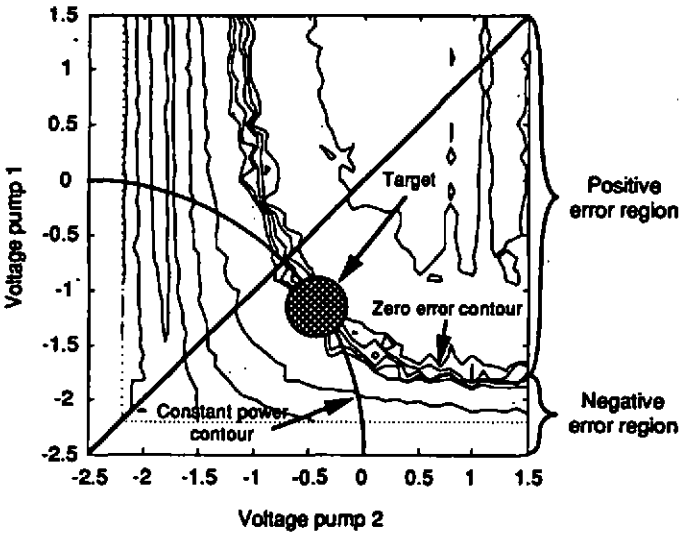


Figure 3: Contour Plot of the Error Surface in the Case of Pressure Gradient

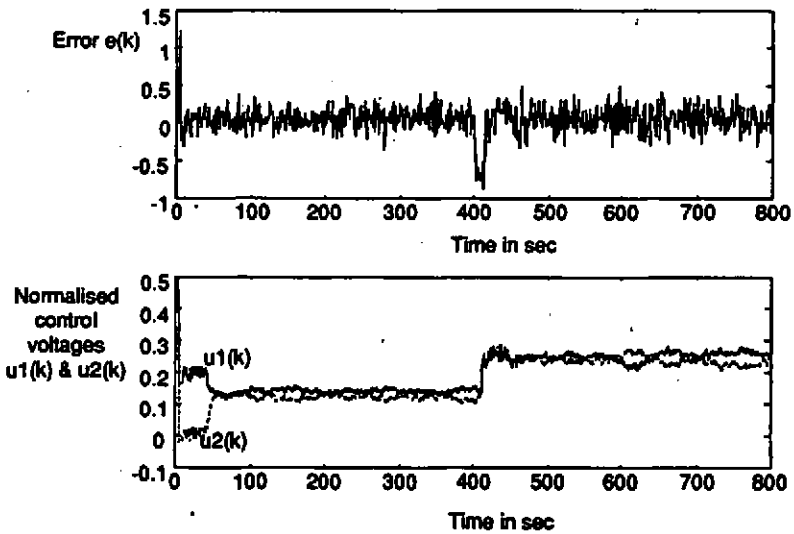


Figure 4: Controller performance and response to a sudden change in mean flow speed at time = 400, in the case of the flat plate without pressure gradient.

## AUTOMATIC CONTROL OF BOUNDARY LAYER TRANSITION

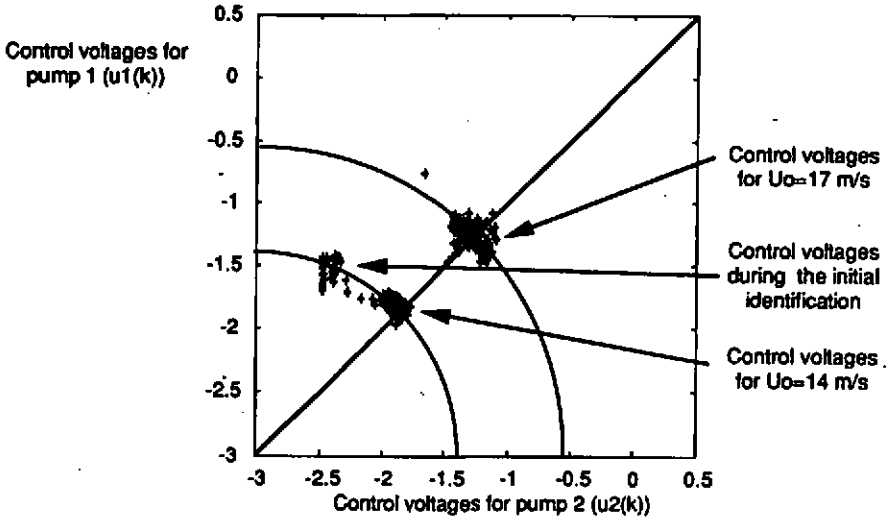


Figure 5: Instantaneous values of the control inputs (+) during convergence to the optimal solution, in the case of the flat plate without pressure gradient .

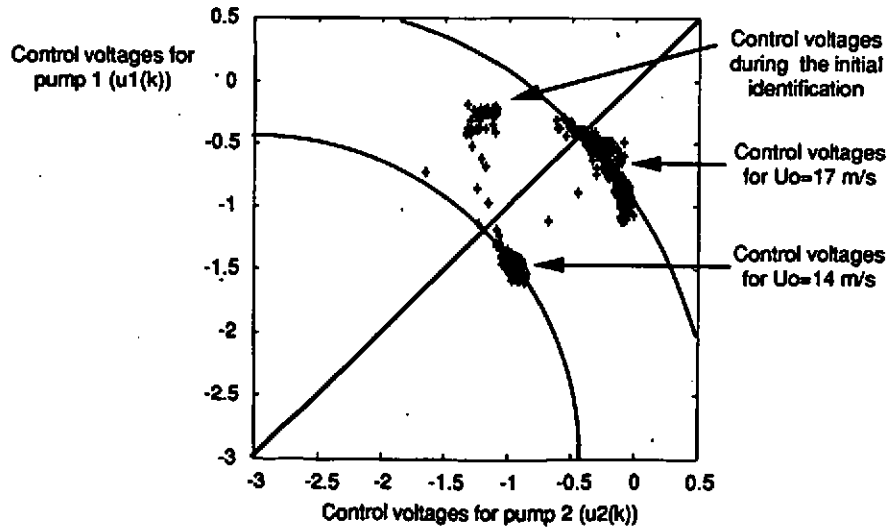


Figure 6: Instantaneous values of the control inputs (+) during convergence to the optimal solution, in the case of the flat plate with pressure gradient.